Water Practice & Technology

IWA PUBLISHING

Water Practice & Technology Vol 16 No 4, 1421 doi: 10.2166/wpt.2021.080

Study on the effect of morphological changes of bridge piers on water movement properties

Xianqi Zhang[a,b,c], Tao Wang[a,*] and Bingsen Duan[a]

[a] Water Conservancy College, North China University of Water Resources and Electric Power, Zhengzhou 450046, China
[b] Collaborative Innovation Center of Water Resources Efficient Utilization and Protection Engineering, Zhengzhou 450046, China
[c] Technology Research Center of Water Conservancy and Marine Traffic Engineering, Zhengzhou, Henan Province 450046, China
*Corresponding author. E-mail: 1124149584@qq.com

ABSTRACT

The different shapes of bridge piers across rivers have a great influence on the river water movement, and the study of the influence of pier morphology changes on the water movement characteristics is of great value for bridge design and river flooding. The hydrodynamic model can effectively simulate and predict the changes of river flow patterns, which can provide scientific data support for river management. This paper constructs a hydrodynamic model based on MIKE21 and applies it to the numerical simulation of river hydrodynamics in the lower reaches of the Yellow River, taking elliptical piers as an example, and simulates the effect of the change of pier morphology on the flow velocity, water level and flow field of the river. The results show that the effect of elliptical pier morphology on the flow characteristics of the river channel is significant; under the same flow rate, the congestion value of the pier at the maximum axis ratio is 1.65 times the minimum axis ratio, and the larger the axis ratio, the more serious the congestion; the difference in flow velocity at the maximum axis ratio can reach 2.33 times the minimum axis ratio.

Key words: bridge pier axial ratio, flow regime, MIKE21 flow model, numerical simulation, Yellow River

HIGHLIGHTS

- This paper uses MIKE21 numerical simulation to analyze and study the changes in river congestion and flow patterns caused by bridge construction, and to provide more practical simulation data for the construction of cross-river bridges.
- The Nash efficiency coefficient of 0.94 is highly accurate in the model validation and evaluation.

1. INTRODUCTION

The existence of piers of cross-river bridges leads to the reduction of the effective water crossing area of the river, and the impact of water flow and vortex generated by the piers blocking the flow, resulting in local water flow with strong turbulence and high flow velocity near the piers, resulting in the phenomenon of congestion before the bridge. Therefore, it is necessary to analyze the river congestion and flow changes caused by the bridge construction before the project implementation (Tang 2014; Luo *et al.* 2015; Hai & Wei 2018). Currently, scholars at home and abroad have conducted a large number of related studies on the impact of cross-river bridges on river channels and achieved more fruitful results. (Yang & Frangopol 2019) conducted a hydrological simulation assessment of long-term regional bridge scour risk based on physical climate change and applied it in the Lihay River basin; Tewodros & Abdusselam (2019) used the MIKE21 FM model to assess the risk of bridge scour in the Ayama basin in Turkey, modeling the effect of urbanization on flood risk in the Ayamama basin, Istanbul; Costabile *et al.* (2015) comparatively analyzed the backwater effects of bridge and no-bridge scenarios based on 1D and 2D river flood models; Dimitriadis *et al.* (2016) comparatively assessed the uncertainty in flood mapping based on 1D and quasi-2D hydraulic models; Zhang *et al.* (2021), based on MIKE21FM model, simulated the effect of different shaped piers on the flow regime of the river; Echeverribar *et al.* (2019) provided a robust two-dimensional model for simulating flood events, which has the ability to avoid instability and makes the model suitable for numerical correction of complex phenomenon simulations; Wang & Jing (2019) studied the effect of bridge piers on flood hazards in the Jialing River basin using the MIKE21 two-dimensional numerical model. Liu *et al.* (2020) based a two-dimensional hydrodynamic model with dynamic numerical simulation of the

congestion and scour generated by the current bridge and the bridge to be reconstructed; Yan *et al.* (2020) studied the pier front congestion and section average congestion characteristics of double piles under different diameters and flow velocity conditions based on the principle of momentum conservation and hydrodynamic model; Yu & Zhu (2019) used the Reynolds time-averaged N-S equation and the standard k-ε turbulence model to investigate the local scour of a series of double-cylindrical piers. Zhang *et al.* (2020) simulated the local scour of cylindrical bridge piers using Flow-3D hydrodynamic and sediment modules. As can be seen from the above, domestic and foreign scholars' research on the influence of river bridges on river channels mainly focuses on the study of river congestion before and after the construction of bridge piers in actual projects, but there is a lack of systematic analysis of the influence of the change of bridge pier axis ratio on river congestion characteristics. The paper aims to build a hydrodynamic model of the lower Yellow River by establishing a two-dimensional mathematical model and simulating the effect of the change of axle ratio on the flow velocity, water level and flow field of the river by taking the elliptical bridge pier as an example. It provides theoretical support for river flooding and navigation.

2. BASIC PRINCIPLES AND METHODS

The MIKE21 model is a two-dimensional mathematical simulation software developed by the Danish Institute of Hydrodynamics (DHI), which is applied to numerical simulation of water flow and water environment in estuaries, bays and marine nearshore areas (Wan & Li 2018), and is one of the more advanced models in the international arena. Its Flow Model hydrodynamic model uses the unstructured grid finite volume method to solve the two-dimensional shallow water equations. The vertical averaged water flow factors are used as the study object to simulate and calculate the planar flow field and its variation (Wang *et al.* 2020; Yan *et al.* 2020; Yuan *et al.* 2020).

2.1. The governing equation

The model uses two-dimensional shallow water equations in the plane to describe the movement of water in the river, and the controlling equations of the numerical water flow model are in the following form in the Cartesian coordinate system (Xu 2010; Bates *et al.* 2015).

Flow continuity equation was defined as follows:

$$\frac{\partial \zeta}{\partial t}+\frac{\partial p}{\partial x}+\frac{\partial q}{\partial y}=\frac{\partial d}{\partial t} \tag{1}$$

X direction momentum equation was defined as follows:

$$\begin{aligned}&\frac{\partial P}{\partial t}+\frac{\partial}{\partial x}\left(\frac{P^2}{h}\right)+\frac{\partial}{\partial y}\left(\frac{pq}{h}\right)+gh\left(\frac{\partial \xi}{\partial x}\right)+\frac{gp\sqrt{p^2+q^2}}{C^2h^2}\\&-\frac{1}{\rho}\left[\frac{\partial}{\partial x}(h\tau_{xx})+\frac{\partial}{\partial y}(h\tau_{xy})\right]-\Omega q-fVV_x+\frac{h}{\rho}\frac{\partial}{\partial x}p_a=0\end{aligned} \tag{2}$$

Y direction momentum equation was defined as follows:

$$\begin{aligned}&\frac{\partial P}{\partial t}+\frac{\partial}{\partial y}\left(\frac{P^2}{h}\right)+\frac{\partial}{\partial x}\left(\frac{pq}{h}\right)+gh\left(\frac{\partial \xi}{\partial y}\right)+\frac{gp\sqrt{p^2+q^2}}{C^2h^2}\\&-\frac{1}{\rho}\left[\frac{\partial}{\partial y}(h\tau_{yy})+\frac{\partial}{\partial y}(h\tau_{xy})\right]-\Omega q-fVV_y+\frac{h}{\rho}\frac{\partial}{\partial y}p_a=0\end{aligned} \tag{3}$$

In those equations,

$$f=2\omega\sin\varphi \tag{4}$$

where, ξ is the free surface water level(m); x and y are spatial coordinates (m); p and q are the flux density in x and y direction respectively (m^2/s); d is the depth change with time(m); g is the acceleration of gravity (m^2/s), which is 9.8 m^2/s; C is the Chezy coefficient ($m^{1/2}/s$); ρ *i*s the water density (kg/m^3); τ_{xx}, τ_{xy} and τ_{yy} are the horizontal shear stress in x direction and the vertical shear stress in x direction, and the vertical shear stress in y

direction respectively (P_a); Ωq is the Coriol coefficient; f is the drag coefficient; V, V_x and V_y are the wind velocity and the wind velocity in x and y direction respectively(m/s); and P is the atmospheric pressure (P_a).

This study aimed at calculating the discrete solution of two-dimensional shallow water governing equations with finite volume method based on unit center.

2.2. Simulation process

(1) Data pre-processing: use RS to extract the topographic elevation values of the river in the study area, import the datum points with elevation in the calculation area, generate a triangular grid from them, and adapt the shape of the bridge pier to improve the calculation accuracy by using the grid encryption method near the bridge pier (Mao *et al.* 2018).
(2) Set up each boundary code, set the upstream boundary of the river as open boundary code1, the downstream boundary of the river as open boundary code2, and the boundary of both banks as closed boundary code3.
(3) Set model parameters: edit each time item needed for model calculation: start time, step number and step length; edit each initial condition of the model: initial river surface elevation, initial flow velocity, etc.; edit model boundary conditions: type and value of upstream and downstream import/export boundaries, etc.; edit each related variable: roughness value and eddy viscosity coefficient, etc.
(4) Export the results to be observed by the model, including river surface elevation, river depth, flow velocity, and direction of flow in the section near the bridge pier, etc.

2.3. Simulation effect evaluation

The simulation effect evaluation index is the Nash efficiency factor NSE, which is defined as:

$$NSE = 1 - \frac{\sum_{t=1}^{N} (y_t - \bar{y}_t)^2}{\sum_{t=1}^{N} (y_t - \mu_t)^2} \tag{5}$$

where, y_t is the actual value at time t; $\bar{y}_t$ is the predicted value at time t; μ_t is the total average value of observations at time t.

3. EXAMPLE ANALYSIS

3.1. Data source

Luokou hydrological station is a national basic water level station built in the lower reaches of the Yellow River, which is 220 kilometers away from the mouth of the Yellow River, and is a national key flood reporting station. Luokou hydrological station is located about 28.9 km upstream of the studied river section, and there is no large tributary inlet from the hydrological station to the studied river section, which has little influence on the average daily flow, so the station is chosen as the basic station for this study. The hydrological information of 2000–2019 years used in this paper mainly comes from the actual measurement data of the Yellow River Network of the Yellow River Conservancy Commission of the Ministry of Water Resources on Luokou hydrological station. The projected coordinate system Xian80-117E is taken as the coordinate system of the study area. The water level-flow relationship of the hydrological stations to be selected is shown in Figure 1.

3.2. Study area

The proposed Jinan Bridge project is selected as the background of numerical simulation, which is located in the lower Yellow River section from Luokou to Lijin, Jinan City, Shandong Province, 28.9 kilometers upstream from Lukou hydrological station, 9.1 kilometers downstream from Liujiayuan water level station, and 0.5 kilometers downstream of the Yangjiagou section in the lower Yellow River test section ditch. The normal direction of the bridge axis within the river channel is basically the same as the flooding direction of the river channel, and the river bend is restricted after artificial treatment. The river potential is stable and the flow is stable due to the bank control project, and the river potential is upward and downward with the change of flow size. The location map of the study area is shown in Figure 2.

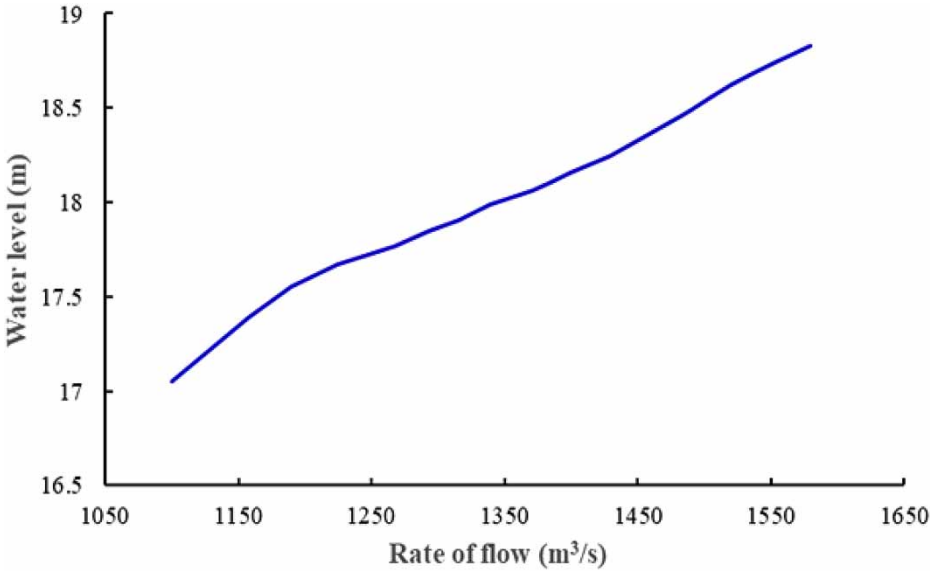

Figure 1 | Water level and flow relationship curve of Luo kou hydrological station from 2000 to 2019.

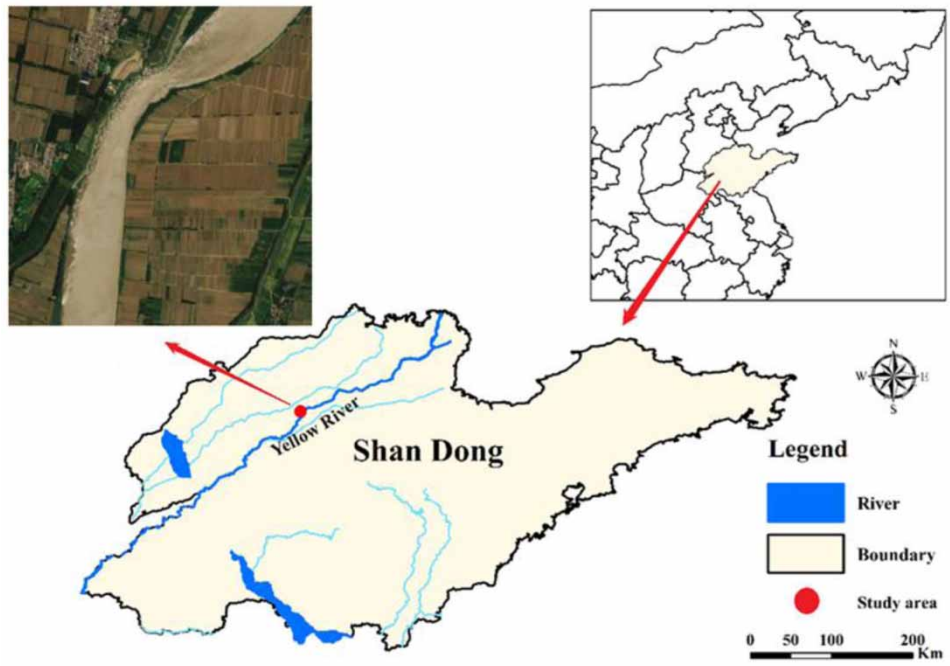

Figure 2 | Location map of the study area.

3.3. Working condition setting

A proposed bridge across the Yellow River is located in the northeastern part of Jinan City, and it is planned to build elliptical piers. In order to analyze the effect of the change of the axial ratio on the water flow characteristics of the river, six scenarios are set for the ratio of short to long axes of elliptical piers: a:b is 1, 0.85, 0.75, 0.5, 0.25, 0.15.

3.4. River segment grid division

The two-dimensional model is constructed by combining the characteristics of the simulated river section, and the simulated area is 5.3 kilometers. the cross-river bridge is arranged symmetrically with the flow direction using double piers, and the simulated river section is divided with a triangular grid, and the grid size is increased appropriately to reduce the model calculation time in the location where the elevation change is not large and the shoreline is smooth; the grid size is increased appropriately in the vicinity of the river section where the project is

located and the location where the elevation change is more drastic or the local topography is abruptly changed, in order to ensure the calculation accuracy. At the same time, in consideration of the relatively small size of the bridge piers after the construction of the bridge, the existence of piers on the beach was not considered in the calculation, the location of the piers near the encrypted edge length of 2 meters, the number of grids is 13265. The grid division diagram is shown in Figure 3.

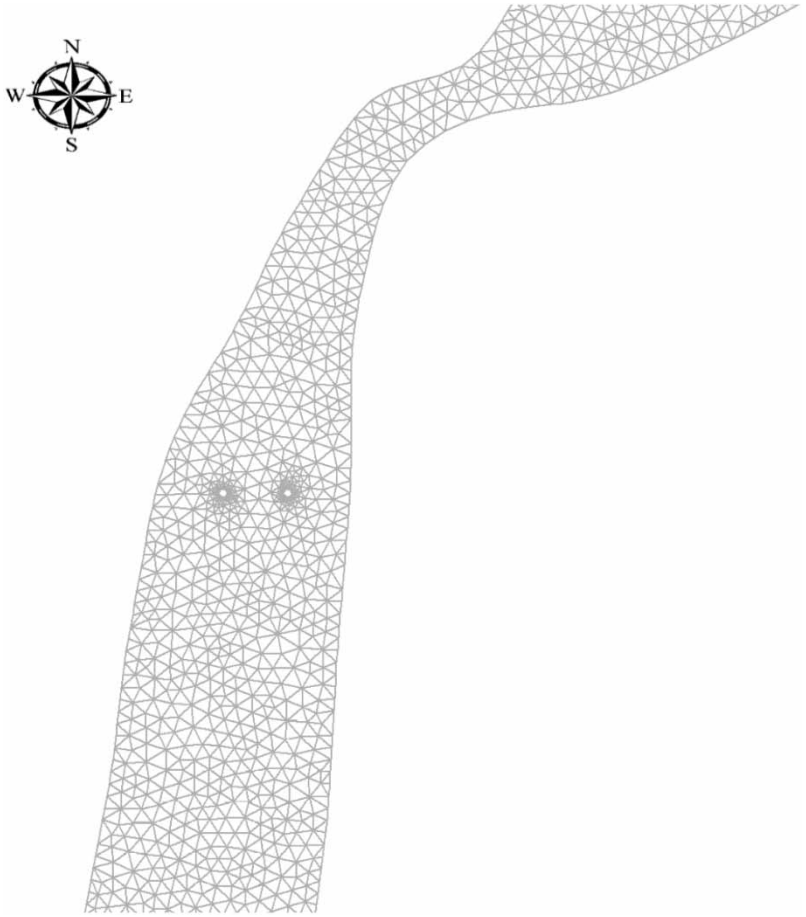

Figure 3 | Grid division diagram.

3.5. Boundary condition setting

In this paper, the MIKE21 hydrodynamic model is used to predict the flow regime at the river abutments. The boundary conditions of the free surface are set as pressure boundary bars, $P = \text{Pa}$ (atmospheric pressure) and $F = 0$ (filled with air); the upstream entrance of the model is set as flow boundary conditions, the downstream exit is set as water level boundary conditions, and the downstream exit of the river channel is set as water level boundary conditions. The calculation grid is divided into three categories: dry, wet and semi-dry; dry grid when the grid water depth $h < h_1$, h_1 can be taken as 0.005 meters; semi-dry grid when the grid water depth $h_1 < h < h_2$, only flow flux but no momentum flux at the interface of adjacent cells, h_2 is taken as 0.1 meters; wet grid when the grid water depth $h > h_2$.

Simulations were carried out separately for elliptical piers with different axial ratios at different flows according to the study context. The changes in the hydraulic elements such as river congestion values and flow regimes are analysed as shown in Table 1.

3.6. Model parameter calibration

The average measured flow information of 2000, 2005, 2010, 2015 and 2019 at Luokou hydrological station was used for the model rate determination, and the alongstream water level information investigated under this flow was used for the two-dimensional mathematical model calculation with the upstream flow and downstream water level of the river as the boundary conditions. The rate determination of the model was carried out.

Table 1 | Simulated working conditions

Work conditions	Axial ratio	Upstream boundary flow/(m^3/s)	Downstream water/m
A1	1	9600 (once in a decade)	22.66
A2		1390(multi-year average)	17.24
A3		295 lowest water level($P = 95\%$)	16.65
B1	0.85	9600 (once in a decade)	22.66
B2		1390(multi-year average)	17.24
B3		295 lowest water level($P = 95\%$)	16.65
C1	0.75	9600(once in a decade)	22.66
C2		1390(multi-year average)	17.24
C3		295 lowest water level($P = 95\%$)	16.65
D1	0.5	9600(once in a decade)	22.66
D2		1390(multi-year average)	17.24
D3		295 lowest water level($P = 95\%$)	16.65
E1	0.25	9600(once in a decade)	22.66
E2		1390(multi-year average)	17.24
E3		295 lowest water level($P = 95\%$)	16.65
F1	0.15	9600(once in a decade)	22.66
F2		1390(multi-year average)	17.24
F3		295 lowest water level($P = 95\%$)	16.65

According to the calculation results, the simulation results are basically consistent with the measured data of the cross section, the Nash efficiency coefficient is 0.94, and the simulated water level matches with the actual water level with high accuracy. After model validation, the model parameters are taken as follows.

(1) Turbulent viscosity coefficient. The turbulent viscosity coefficient of this model is directly assigned according to the recommended value of the U.S. Waterways Experiment Station, which is taken as 2 400 Pa-s. The turbulent viscosity coefficient in each direction of the calculation is taken as the same value.
(2) Roughness rate determination. The river roughness is actually a comprehensive resistance coefficient, which reflects the combined effects of bed and bank resistance, channel morphology changes, current resistance and channel topography generalization of the calculated river section. In this paper, according to the calculation conditions in Table 2, the turbulent viscosity coefficient is selected to the value of 2 400 Pa.s, given the inlet boundary flow and water level at the outlet, and the channel roughness is determined by fitting the water level at the inlet. The Nash efficiency coefficient is 0.95, and the model has high calculation accuracy. The riverbed roughness is 0.033 and the eddy viscosity coefficient is 0.28. The simulation period is 2.5 h and the time step is 30 s.

Table 2 | Model validation of measured data

Level year	Measured flow rate/(m^3/s)	Measured water level/m	Model calculation/m	Nash coefficient R_{NS}
2000	1,371	18.06	18.04	0.94
2005	1,580	18.83	18.85	
2010	1,225	17.67	17.64	
2015	1,110	17.05	17.06	
2019	1,490	18.49	18.53	

4. SIMULATION RESULTS AND ANALYSIS

According to the calculation scheme of the river under different working conditions for different axial ratio elliptical bridge pier situation for quantitative analysis, in order to facilitate the comparison of the river congestion and flow velocity changes under different piers, in the bridge axis layout detection section, section and the river flow direction perpendicular, the first monitoring point is arranged in the left bank of the river, a total of

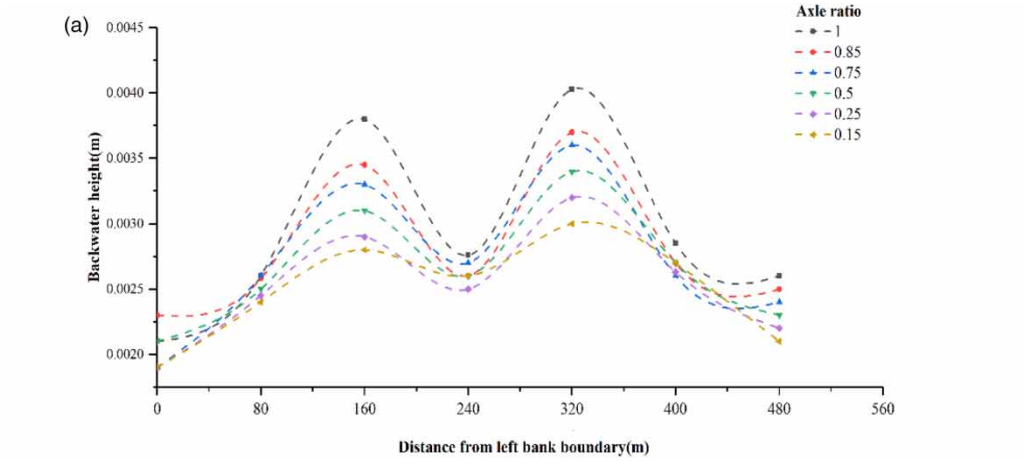

Variation of congestion height and shaft ratio at the lowest water level flow (P=95%)

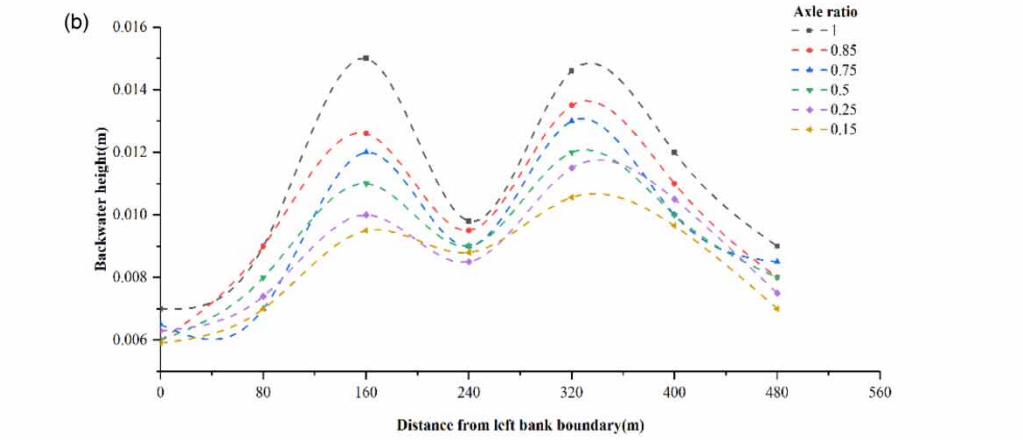

Variation of congestion height and shaft ratio under multi-year average flow conditions

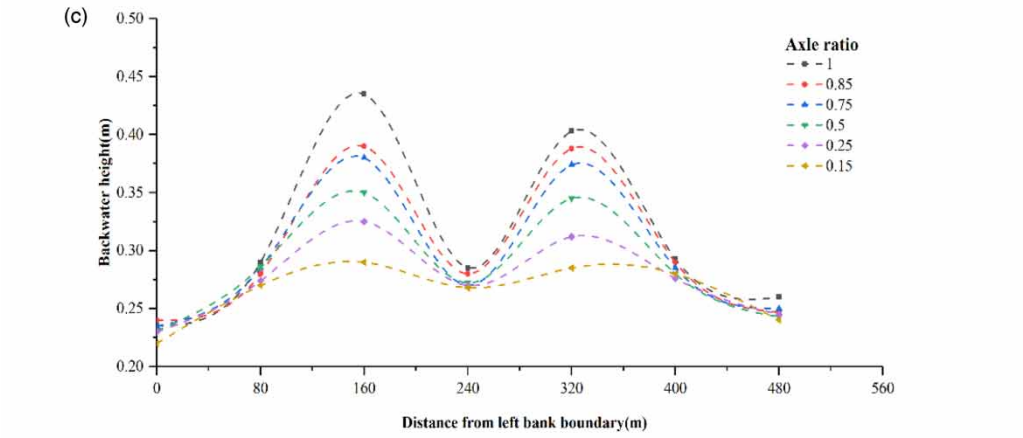

Variation of congestion height and axial ratio under 1-in-10-year flow conditions

Figure 4 | Variation of congestion height and axial ratio under different flow rates. (a) Variation of congestion height and shaft ratio at the lowest water level flow ($P = 95\%$). (b) Variation of congestion height and shaft ratio under multi-year average flow conditions. (b) Variation of congestion height and axial ratio under 1-in-10-year flow conditions.

seven monitoring points, each monitoring point spacing was 80 meters, the bridge pier is located at the third and fifth monitoring points.

4.1. Relationship between congestion height and flow

When the axial ratio of elliptical piers is changed, the water flow changes with the change of the axial ratio and the water surface also changes. In order to analyze the relationship between congestion height and axial ratio, the

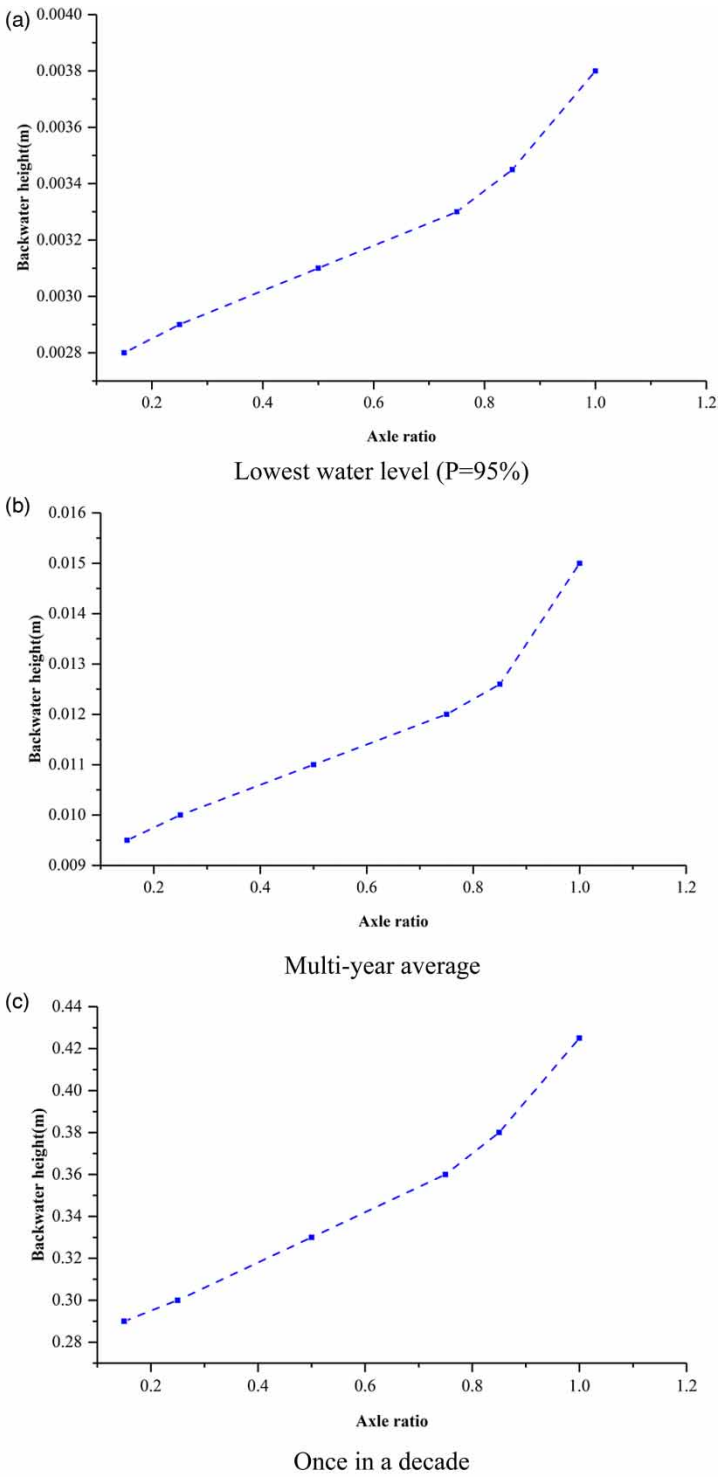

Figure 5 | Influence of axial ratio change on congestion near bridge piers. (a) Lowest water level ($P = 95\%$). (b) Multi-year average. (c) Once in a decade.

numerical simulation results of congestion values of elliptical piers at different axial ratios are shown in Figure 4. From the figure, it can be seen that the congestion height ΔZ increases with the increase of axial ratio, and the congestion increases significantly near the piers. Therefore, it is necessary to consider the influence of the change of the axial ratio of elliptical piers in the study of flood control of water-related projects.

In order to explore the effect of the change of axial ratio on the congestion height of elliptical piers, six axial ratios were used to calculate the maximum congestion height and the change of axial ratio as shown in Figure 4. At a large shaft ratio of 0.75, a significant increase in the congestion height is observed.

4.2. Analysis of the flow field around the bridge pier

When the bridge pier is in the river channel, the water flow within the range of the bridge pier layout is in the influence of the pier, asymmetric velocity changes, and the local range of near-shore flow velocity increase will cause the water to intensify the river bank scour. To explore the elliptical bridge pier different axis ratio arrangement caused by the flow field, the said distribution law is important in accordance with the boundary conditions; the annual average water level near the bridge pier under different water level conditions flow velocity change diagram is shown in Figure 5.

By analyzing the flow velocity of the river in the bridge area, it can be concluded that under the blocking effect of the bridge pier, the water flowing through the bridge pier appears as eddies and backflow, and the flow velocity decreases significantly; the magnitude of the flow velocity change increases with the increase of the axial ratio, and the flow velocity change decreases significantly in the vicinity of the bridge pier.

Table 3 shows that the maximum axial ratio flow velocity changes are 1.57, 1.87 and 2.33 times the minimum axial ratio under the conditions of 1-in-10-year, multi-year average and minimum water level flow; the flow velocity changes mainly occur near the piers of the main channel, and the average overall increase in flow velocity at the banks of both sides is relatively small, and the flow direction tends to be consistent with the river course.

Table 3 | Variation of water surface flow velocity at the bridge pier

Axis ratio	Once in a decade	Multi-year average	Minimum water level ($P = 95\%$)
1	0.500	0.186	0.09
0.85	0.409	0.17	0.085
0.75	0.388	0.167	0.085
0.5	0.311	0.142	0.076
0.25	0.268	0.112	0.064
0.15	0.210	0.099	0.057

According to the boundary conditions, the flow field near the bridge pier under the multi-year average flow conditions is shown in Figures 6 and 7. As can be seen from the figure, the direction of river flow velocity and the direction of basic water flow, in the vicinity of the bridge pier side and rear by the influence of bypass scour, the larger the axis ratio, the greater the impact, and the river potential of the river channel caused by a certain impact; in addition to the local existence of disturbance flow at the bridge pier, the flow of water flow is relatively smooth, causing changes in the flow line on both sides of the river inner embankment slope. The impact is small.

Under the other 2 flow conditions, the flow pattern is basically the same, and the direction of river flow velocity is basically the same as the flow direction, and the influence of bypass scour at the back of the side near the bridge pier and the influence of the axis ratio on the flow field is the same as the flow field change under the multi-year average flow.

5. CONCLUSION

In this paper, based on the MIKE21 hydrodynamic model, the effect of elliptical piers with different axial ratios on the river flow was analyzed and the following conclusions were obtained.

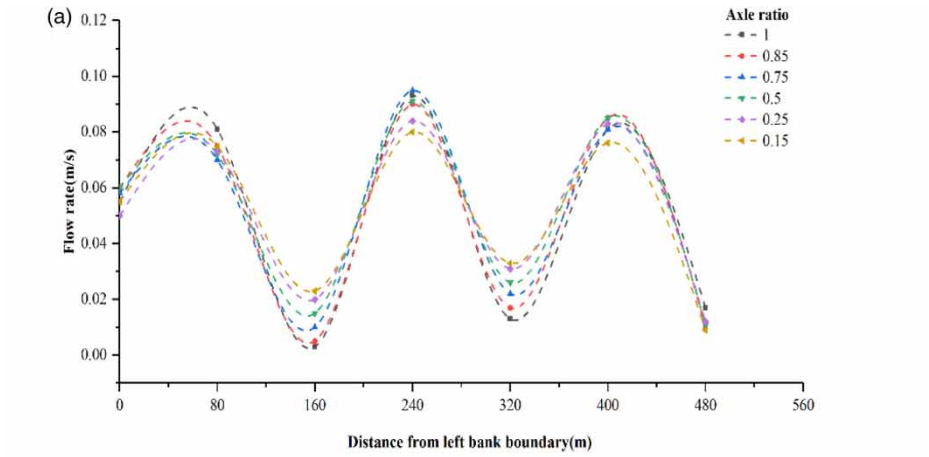

Variation of flow rate and shaft ratio under the lowest water level flow (P=95%)

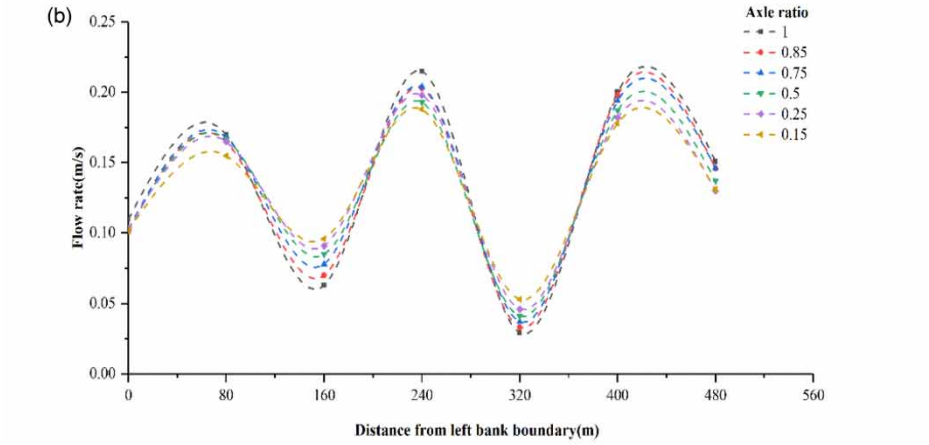

Variation of flow rate and shaft ratio under multi-year average flow conditions

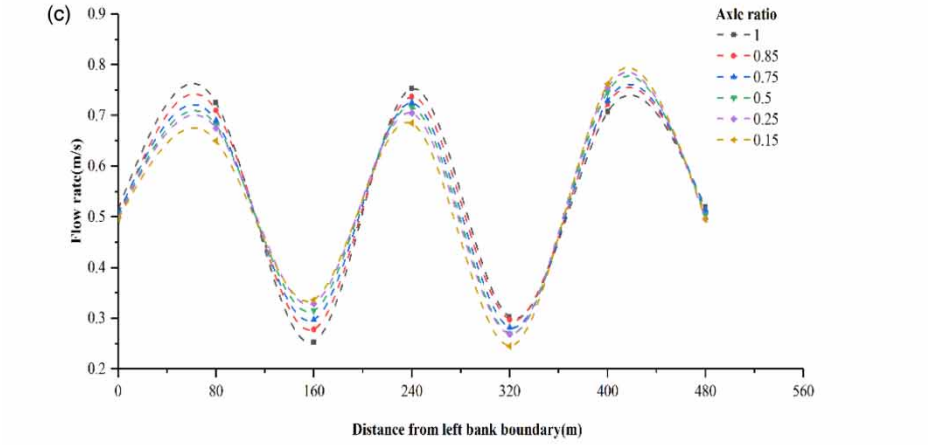

Variation of flow velocity and axial ratio under the decadal flow condition

Figure 6 | Variation of flow velocity and axial ratio under different flow rates. (a) Variation of flow rate and shaft ratio under the lowest water level flow ($P = 95\%$). (b) Variation of flow rate and shaft ratio under multi-year average flow conditions. (c) Variation of flow velocity and axial ratio under the decadal flow condition.

(1) Using MIKE21 hydrodynamic model, numerical simulations, pre-pier congestion and flow velocity changes were analyzed and compared under different flow rates for different axial ratios of elliptical piers respectively, and the results showed that: the change of axial ratio of elliptical piers had different effects on the flow pattern

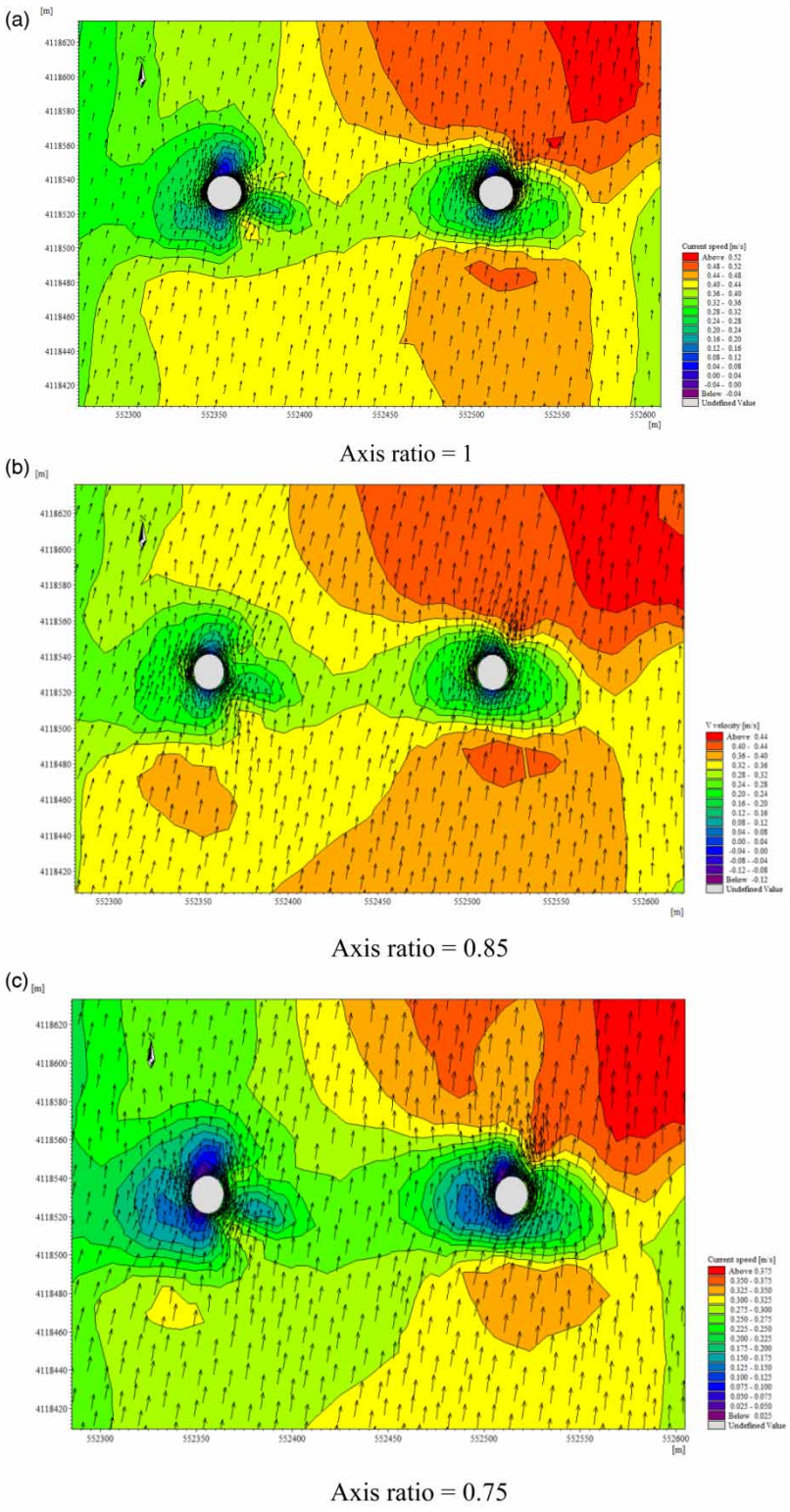

Figure 7 | Variation of flow field of elliptical bridge pier with different axis ratios under multi-year average flow. (a) Axis ratio = 1. (b) Axis ratio = 0.85. (c) Axis ratio = 0.75. (d) Axis ratio = 0.5. (e) Axis ratio = 0.25. (f) Axis ratio = 0.15. *(Continued.)*

of the river, and the height of pre-pier congestion and flow velocity increased significantly with the increase of axial ratio, which had certain effects on the river potential.

(2) The two-dimensional hydrodynamic numerical model of the simulated river section matches with the measured river hydrology and topographic data, and the Nash efficiency coefficient meets the accuracy requirements in model verification and evaluation. Based on the MIKE21 hydrodynamic model, the

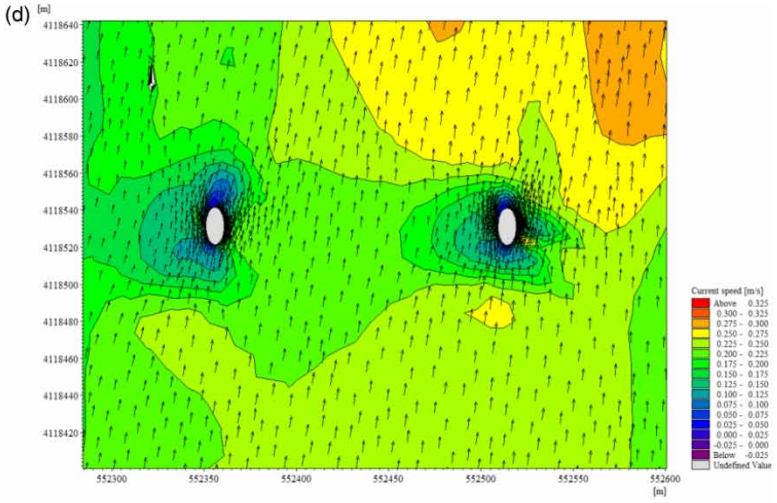

(d) Axis ratio = 0.5

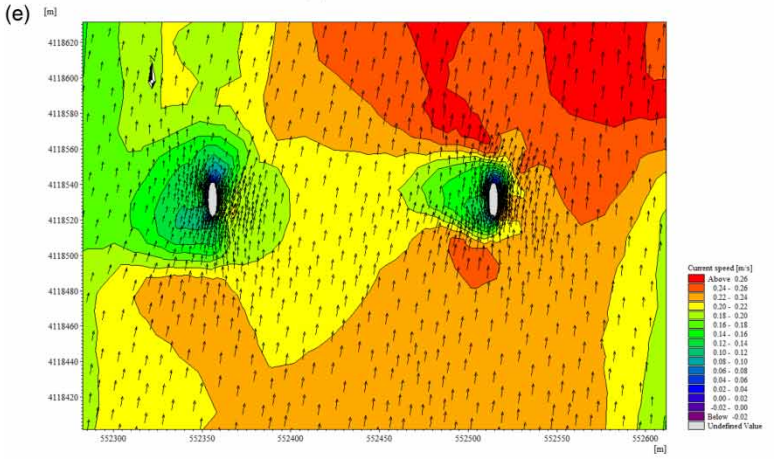

(e) Axis ratio = 0.25

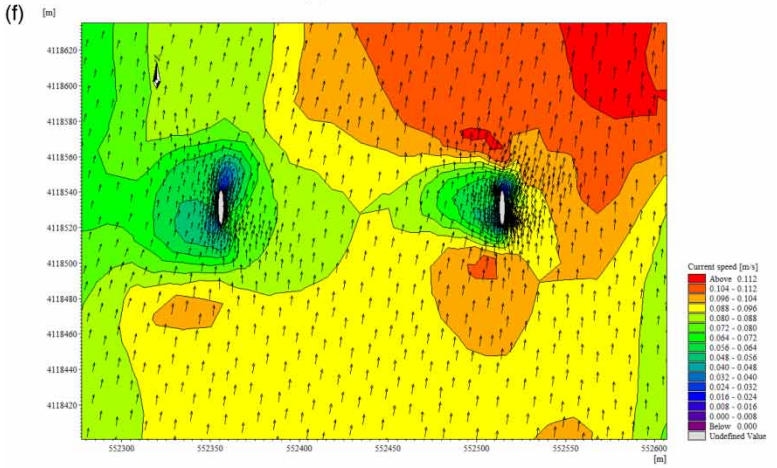

(f) Axis ratio = 0.15

Figure 7 | Continued.

simulation calculates the changes of river flow and congestion values, and the results are reasonable and have high practical value for the construction of cross-river bridges.

(3) The model uses constant flow conditions to simulate a section of the lower Yellow River without considering the non-constant flow factors, and the simulation results may deviate from the actual one. In the future, we can further simulate several representative river sections to compare and analyze the results, improve the

simulation accuracy, explore the evolution mechanism, and provide better support and reference for the actual construction.

ACKNOWLEDGEMENTS

This work is financially supported by Technology Research Center of Water Environment Governance and Ecological Restoration Academician Workstation of Henan Province, Program for Science & Technology Innovation Talents in Universities of Henan Province.

DATA AVAILABILITY STATEMENT

All relevant data are included in the paper or its Supplementary Information.

REFERENCES

Bates, P. D., Horritt, M. S. & Hervouet, J. M. 2015 Investigating two-dimensional, finite element predictions of floodplain inundation using fractal generated topography. *Hydrological Processes* **12**(8), 1257–1277.

Costabile, P., Macchione, F., Natale, L. & Petaccia, G. 2015 Comparison of scenarios with and without bridges and analysis of backwater effect in 1-D and 2-D river flood modeling. *CMES-Computer Modeling in Engineering & Sciences* **109–110**(2), 81–103.

Dimitriadis, P., Tegos, A., Oikonomou, A., Pagana, V., Koukouvinos, A., Mamassis, N., Koutsoyiannis, D. & Efstratiadis, A. 2016 Comparative evaluation of 1D and quasi-2D hydraulic models based on benchmark and real-world applications for uncertainty assessment in flood mapping. *Journal of Hydrology* **534**, 478–492.

Echeverribar, I., Morales-Hernández, M., Brufau, P. & García-Navarro, P. 2019 2D numerical simulation of unsteady flows for large scale floods prediction in real time. *Advances in Water Resources* **134**, 103444.

Hai, X. S. & Wei, P. L. 2018 Numerical simulation of turbulent width of square bridge pier in curved river channel. *Water Transport Engineering* **2018** (01), 134–141.

Liu, X. C., Geng, P. C., Cao, L. & Sun, X. L. 2020 Mike21 simulates the influence of cross-river bridge on river regime. *People's Yellow River* **42**(S1), 24–25 + 29.

Luo, W. G., Lu, J. & Lai, H. 2015 Research on the backwater in front of multiple parallel bridge piers at equal distances. *Journal of Sichuan University: Engineering Science Edition* **47**(4), 6–13.

Mao, M. X., Huang, H. M. & Wang, Y. G. 2018 Effects of grid size on numerical simulation of river hydrodynamics [J]. Influence of grid size on numerical simulation of river hydrodynamics. *Water Transport Engineering* **2018** (3), 135–142.

Tang, Y. H. 2014 Application of TUFLOW in simulating the impact of bridge piers on flooding evaluation. *Hydropower Energy Science* **32**(02), 55–59.

Tewodros, A. N. & Abdusselam, A. 2019 Modeling the effect of urbanization on flood risk in Ayamama Watershed, Istanbul, Turkey, using the MIKE 21 FM model. *Natural Hazards* **99**(2), 1031–1047.

Wan, L. M. & Li, P. J. 2018 Numerical simulation of navigable flow conditions of bridges across rivers. *Water Conservancy Science and Technology and Economy* **24**(02), 28–33.

Wang, W. & Jing, H. 2019 Effects of bridge piers on flood hazards: a case study on the Jialing river in China. *Water* **11**(6), 1181.

Wang, Q. N., Peng, W. Q., Dong, F. & Nan, O. 2020 Simulating flow of an urban river course with complex cross sections based on the MIKE21 FM model. *Water* **12**(3), 761–781.

Xu, T. 2010 Overview of Danish MIKE21 model and application examples. *Water Technology and Economics* **16**(08), 867–869.

Yang, D. Y. & Frangopol, D. M. 2019 Physics-based assessment of climate change impact on long-term regional bridge scour risk using hydrologic modeling: application to Lehigh River watershed. *Journal of Bridge Engineering* **24**(11), 1–13.

Yan, J. C., Xu, H. & Jiao, Z. X. 2020 Prediction and numerical simulation of bridge pier congestion based on conservation of momentum. *People's Changjiang* **51**(S2), 280–284.

Yu, P. & Zhu, Z. W. 2019 Refinement of local scour simulation for tandem double cylindrical bridge piers. *Chinese Journal of Highways* **32**(01), 107–116.

Yuan, X. Y., Feng, S. L., Wang, Z. K., Xu, W. & Si, L. C. 2020 Two-dimensional numerical simulation of the effect of bridge pier shape on water flow. *People's Yellow River* **42**(S2), 37–39 + 42.

Zhang, S. G., Yin, J. B. & Zhang, G. G. 2020 Flow-3D-based simulation of local scour large eddies for cylindrical bridge piers. *Sediment Research* **45**(01), 67–73.

Zhang, X. Q., Wang, T. & Lu, X. B. 2021 Influence of bridge piers shapes on the flow of the lower Yellow River. *Water Practice & Technology* **16**(2), 661–680.

First received 10 May 2021; accepted in revised form 2 August 2021. Available online 16 August 2021